Nat Hazards
DOI 10.1007/s11069-016-2344-7

ORIGINAL PAPER

GPS geodetic infrastructure for natural hazards study in the Puerto Rico and Virgin Islands region

Linqiang Yang[1] · Guoquan Wang[1] · Victor Huérfano[2] · Christa G. von Hillebrandt-Andrade[3] · Jose A. Martínez-Cruzado[4] · Hanlin Liu[1]

Received: 5 September 2015 / Accepted: 27 April 2016

Abstract The Puerto Rico and Virgin Islands (PRVI) are located within the complex plate boundary zone between the North American and Caribbean plates. This region faces multiple natural hazards, such as earthquakes, tsunamis, landslides, hurricanes, and flooding. The islands are part of the Greater Antilles island chain, which is one of the earliest places that employed Global Positioning System (GPS) technology in plate tectonics and natural hazards studies. A dense Continuously Operating Reference Stations (CORS) network with 24 permanent GPS stations is currently operated by a joint effort of academic, government, and local land surveying communities. This region has been regarded as one of the densest CORS coverage regions worldwide. This article summarized the current GPS geodetic infrastructure in the PRVI region, which includes three components: a dense CORS network that is open to the public, a stable local reference frame that is updated in time, and sophisticated software packages for GPS data processing that are freely available to the academic and research community. This article focused on establishing a local reference frame, the stable Puerto Rico and Virgin Islands reference frame of 2014 (PRVI14), which is essential for precisely delineating local ground deformation over space and time. Applications of the geodetic infrastructure for precise faulting, landslide, and sea-level monitoring were illustrated in this study. According to this study, the St. Croix Island is moving away from the Puerto Rico and Northern Virgin Islands toward southeast with a steady velocity of 1.7 mm/year; the Lajas Valley in southwestern

✉ Linqiang Yang
lyang18@uh.edu

[1] Department of Earth and Atmospheric Sciences, National Center for Airborne Laser Mapping (NCALM), University of Houston, Houston, TX 77004, USA

[2] Puerto Rico Seismic Network, Department of Geology, University of Puerto Rico at Mayaguez, Mayaguez, PR 00680, USA

[3] US National Weather Service Caribbean Tsunami Warning Program, National Oceanic and Atmospheric Administration (NOAA), Mayaguez, PR 00680, USA

[4] Puerto Rico Strong Motion Program, Department of Civil Engineering, University of Puerto Rico at Mayaguez, Mayaguez, PR 00680, USA

Published online: 09 May 2016

of Puerto Rico may be experiencing a north–south direction extension (1.5 mm/year) and a minor right-lateral strike slip (0.4 mm/year) with respect to the PRVI14 reference frame; the current absolute sea-level rise rate in the PRVI coastal region is about 1.6–2.0 mm/year.

Keywords GPS · Local reference frame · Natural hazards · Puerto Rico · Virgin Islands · Faulting · Landslide · Sea-level rise

1 Introduction

The Puerto Rico and Virgin Islands (PRVI) region is located within the complex plate boundary zone between the North American and Caribbean plates. The North American plate moves westward relative to the Caribbean plate at a rate determined from GPS geodesy of 2 cm/year (Jansma et al. 2000; Calais et al. 2002). The PRVI region is a part of the Greater Antilles island chain, which is located in a 250-km-wide, east–west trending zone of complex transpressional deformation. Geodesy and seismicity data suggest the existence of a Puerto Rico—northern Virgin Islands microplate that is relatively rigid and internally seismically quiescent (Masson and Scanlon 1991; Jansma et al. 2000). The PRVI block is delimited by the Puerto Rico Trench to the north, the Muertos Trough to the south, the Anegada Passage to the east, and the Mona Passage to the west (Masson and Scanlon 1991; Jansma and Mattioli 2005; Benford et al. 2012; Huérfano et al. 2005). The main island of Puerto Rico is a rectangular-shaped island that extends approximately 200 km from east to west and 60 km from north to south. The Virgin Islands are about 100 km east of Puerto Rico and consist of about 80 islands and cays. The PRVI region referred to in this article covers an area of about 40,000 km^2 (Fig. 1). The PRVI region is densely populated,

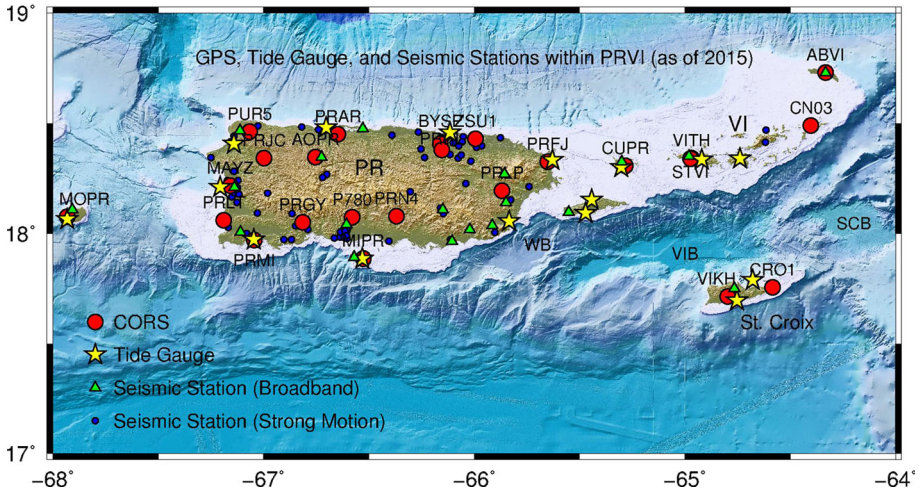

Fig. 1 *Map* showing the locations of current GPS, tide gauge and seismic stations in the Puerto Rico and Virgin Islands region. *PR* represents the Puerto Rico Island, *VI* represents the Virgin Islands, *WB* represents the Whiting Basin, *VIB* represents the Virgin Islands Basin, *SCB* represents the St. Croix Basin

Table 1 Basic information of current 24 CORS in the PRVI region

4-char ID	Location	Longitude (°)	Latitude (°)	Start date	End date	Span (year)	Operator	Monument type	Data archiving
BYSP	Bayamón, PR**	−66.1612	18.40784	May-08	Current	7	UPRM	PBO shallow-drilled braced	UNAVCO
CUPR	Culebra Island, PR**	−65.2825	18.30744	Oct-08	Current	7	UPRM	PBO shallow-drilled braced	UNAVCO/NGS
ABVI	Anegada Island, BVI***	−64.3325	13.72968	Feb-11	current	4	UPRM	PBO shallow-drilled braced	UNAVCO/NGS
MIPR	Caja De Muertos Island, PR**	−66.5270	17.88622	May-08	Current	7	UPRM	PBO shallow-drilled braced	UNAVCO/NGS
MOPR	Mona Island, PR**	−67.9312	18.07690	Oct-08	Aug-11	3	UPRM	PBO shallow-drilled braced	UNAVCO/NGS
AOPP	Arecibo, PR**	−66.7541	18.34653	Sep-08	Current	7	UPRM	PBO shallow-drilled braced	UNAVCO
STVI	St. Thomas Island, USVI***	−64.9745	18.34010	Oct-08	Current	7	UPRM	PBO shallow-drilled braced	UNAVCO/NGS
MAYZ	Mayaguez, PR**	−67.1589	18.21759	Feb-10	Current	5	UPRM	Concrete port-based single-steel pole	UNAVCO/NGS
P780	Ponce, PR**	−66.5791	18.07503	May-08	Current	7	UNAVCO/PBO	PBO shallow-drilled braced	UNAVCO/NGS
CN03	Virgin Gorda, BVI****	−64.4025	18.49046	Feb-13	Current	2	UNAVCO/ COCONET	PBO shallow-drilled braced	UNAVCO
CRO1	St. Croix Island, USVI***	−64.5843	17.75690	Oct-95	Current	20	JPL	Ground-based concrete monolith	UNAVCO/NGS
VITH	St. Thomas Island, USVI***	−64.9692	18.34333	Aug-06	Current	9	NOAA-NGS	Building-based steel pole	NGS
PRMI	Isla Magueyes Island, PR**	−67.0454	17.97040	Mar-06	Current	9	NOAA-NGS	Building-based steel pole	NGS
VIKH	St. Croix Island, USVI***	−64.7981	17.71618	Aug-06	Current	9	NOAA-NGS	Building-based steel pole	NGS
PRJC	San Sebastian, PR**	−66.9995	18.34223	Mar-10	Current	5	HLCM Group, Inc.	Building-based steel pole	NGS
PRLP	Las Piedras, PR**	−65.8683	18.19490	Apr 10	Current	5	HLCM Group, Inc.	Building-based steel pole	NGS
PRN4	Coamo, PR**	−66.3691	18.07859	Mar-09	Current	6	HLCM Group, Inc.	Building-based steel pole	NGS
PRGY	Guayanilla, PR**	−66.8144	18.05095	Mar-10	Current	5	HLCM Group, Inc.	Building-based steel pole	NGS

Table 1 continued

4-char ID	Location	Longitude (°)	Latitude (°)	Start date	End date	Span (year)	Operator	Monument type	Data archiving
PRLT	Cabo Rojo, PR**	−67.1891	18.05984	Feb-09	Current	6	HLCM Group, Inc.	Building-based steel pole	NGS
PRAR	Arecibo, PR**	−66.6474	18.45048	Jun-09	Current	6	HLCM Group, Inc.	Building-based steel pole	NGS
PRFJ	Fajardo, PR**	−65.6514	18.32632	Sep-12	Current	3	HLCM Group, Inc.	Building-based steel pole	NGS
PRHL	Bayamón, PR**	−66.1536	18.38003	May-09	Current	6	HLCM Group, Inc.	Building-based steel pole	NGS
ZSU1/ ZSU4	Carolina, PR**	−65.9935	18.43134	Feb-03	Current	12	FAA*	Ground-based high steel tower	NGS
PUR3/ PUR5	Aguadilla, PR**	−67.0670	18.46298	Feb-97	Current	18	US Coast guard	Ground-based high steel tower	NGS

* *FAA* Federal Aviation Administration; ** *PR* Puerto Rico; *** *USVI* US Virgin Islands; **** *BVI* British Virgin Islands

with almost four million people inhabiting the islands. The integration of geological risks and human settlement makes this region especially vulnerable to natural hazards. This region has a long history of destructive earthquakes, tsunamis, hurricanes, and landslides (McCann 1985; Lander et al. 2002; Pielke et al. 2003; Wang 2012; Wang et al. 2011).

A seismic, tide gauge, and high-rate GPS integrated natural hazards monitoring network (Fig. 1) has been established in the PRVI region by a joint effort of academic, government, and private sectors. The Puerto Rico Seismic Network (PRSN) at the University of Puerto Rico (Mayaguez) is the regional authority for monitoring earthquakes and tsunamis in the PRVI region. The integrated multi-hazard observational network has become a fundamental infrastructure for conducting natural hazards monitoring, research, and education in the PRVI region. A detailed introduction about the seismic monitoring infrastructure can be obtained from Clinton et al. (2006). This study aims to introduce the GPS geodetic infrastructure and its applications for monitoring neotectonic faulting, landslide, and long-term sea-level changes. A mature GPS geodetic infrastructure would include three fundamental components: a network of Continuously Operating Reference Stations (CORS) that is open to the public, a stable local reference frame that is updated in time, and sophisticated software packages for GPS data processing. A precise local reference frame is essential for precisely delineating local ground deformation over time and space. This study aims to establish a stable local reference frame using the long-term (>5 years) GPS observations in the PRVI region.

The term GPS has been replaced by the term "Global Navigation Satellite Systems (GNSS)" in the satellite positioning community. GNSS is used as an umbrella term for all current and future global satellite-based radio navigation systems, such as the United States' NAVSTAR Global Positioning System, Russia's Global Navigation Satellite System (GLONASS), Europe's Galileo, and China's BeiDou satellite positioning systems. Generally, the term GPS is specific to the GNSS controlled by the USA. All the PRVI stations have the capability of recording GLONASS signals. In fact, several PRVI stations are recording GLONASS observations. As of 2015, most applications in natural hazards study primarily rely on the United States' GNSS signals and the most sophisticated software packages (e.g., GIPSY/OASIS, GAMIT/GLOBK) currently only handle GPS signals. It is for this reason that this study uses the term GPS. Only GPS signals were used in this study.

1.1 The PRVI GPS network

GPS stations were installed in the northeastern Caribbean as early as 1986 for the purpose of studying plate tectonics (Dixon et al. 1991). These sites were reoccupied several times in the following years (Dixon et al. 1998). Jansma and Mattioli have maintained a campaign GPS observation network in the PRVI region since the 1990s (Calais et al. 2002; Jansma et al. 2000; Jansma and Mattioli 2005). As of May 2015, there are 24 CORS in the PRVI region that are open to the public (Fig. 1; Table 1). Eight CORS were installed by the Puerto Rico Seismic Network (PRSN) at the University of Puerto Rico at Mayaguez (UPRM). The installation was primarily funded by a National Science Foundation (NSF) Major Research Instrumentation (MRI) project (EAR-0722540). Each UPRM CORS is co-located or closely spaced (<2 km) with a permanent seismic station or a tide gauge station. Daily 15-s sampled raw GPS data are archived at the UNAVCO public data archiving facility (http://facility.unavco.org/data). UNAVCO is a nonprofit university-governed consortium that facilitates geoscience research and education using geodesy. A private surveying company, HLCM Group Inc. (http://www.hlcmgroup.com), also installed eight

CORS in the PRVI region for land surveying applications. All data from these HLCM stations are freely available to the public through the CORS data archiving facility (http://geodesy.noaa.gov/CORS) operated by the National Geodetic Survey (NGS) at the National Oceanic and Atmospheric Administration (NOAA). Several other agencies, such as the US Coast Guard, Federal Aviation Administration (FAA), Jet Propulsion Laboratory (JPL), NGS, and UNAVCO, also operate several continuous GPS stations in the PRVI region (Table 1).

Figure 2 illustrates the site views at four typical PRVI CORS: BYSP, MAYZ, PRAR, and CRO1. BYSP is located in the Bayamón Science Park near San Juan and is co-located with a strong motion seismic station. This site has become a very popular site for conducting K-12 education and outreach activities for earthquake and tsunami hazards education in Puerto Rico. The antenna monument of BYSP is a short-drilled braced GPS monument that was designed by UNAVCO for the Plate Boundary Observatory (PBO) project (UNAVCO 2014). Seven UPRM CORS and the PBO station P780 use the short-drilled braced monument (Yang et al. 2015). MAYZ is located on a concrete platform at the Mayaguez port. It is co-located with a tide gauge station operated by PRSN and

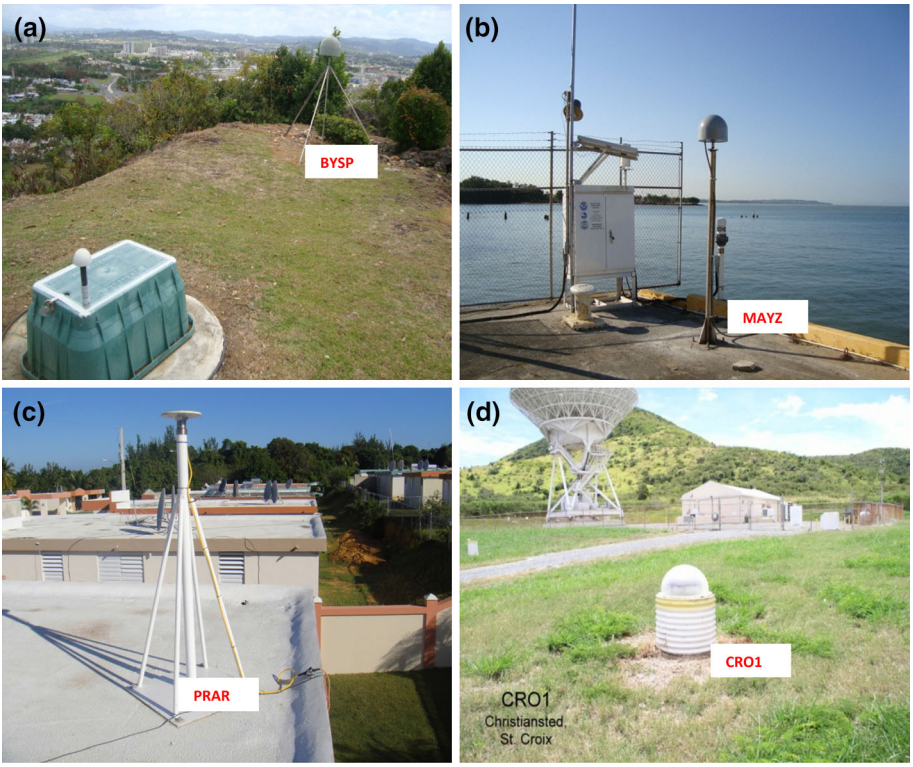

Fig. 2 **a** *A site view* at the GPS (BYSP) and strong motion accelerometer co-located site in the Bayamón Science Park, Bayamón, PR. The antenna monument is the typical PBO short-drilled braced monument designed by UNAVCO. **b** *A site view* at the GPS (MAYZ) and tide gauge co-located site in the Mayaguez port, Mayaguez, PR. **c** A typical building-based GPS station (PRAR) installed by the HLCM Group Inc. in Arecibo, Puerto Rico. **d** *A site view* at the IGS permanent reference station CRO1 (1995–2014) on the St. Croix Island

NOAA. PRAR is located in Arecibo, Puerto Rico. It is a typical building-based CORS installed and operated by the HLCM Group Inc. CRO1 was installed by the Jet Propulsion Laboratory (JPL) in 1995. It has the longest history among the 24 PRVI CORS. JPL is a federally funded research and development center and NASA field center located in Pasadena, California.

1.2 GPS data processing software

Surveying-level GPS units record satellite signals (e.g., pseudo-ranges and phase cycles of L1 and L2 carriers) but do not directly provide high-precision positions. In order to obtain centimeter positional measurements, complex calculations are required. High-precision positions can be calculated in real time or after the data have been collected by post-processing. In general, post-processing achieves higher precision than real-time processing because more information is available for post-processing than for real-time processing (Aponte et al. 2009). Real-time processing techniques are essential for real-time monitoring and early warning of natural hazards, such as landslide monitoring and tsunami early warning. The private land surveying company, HLCM Group Inc., operates a real-time kinematic (RTK) virtual reference station (VRS) network for real-time land surveying (http://hlcmgroup.com/services.html). The RTK VRS system can be adapted to real-time landslide monitoring in this region. The PRSN is in the process of integrating a real-time GPS positioning system into its earthquake monitoring and tsunami early-warning program. Post-processing is often used in the research community. Several sophisticated software packages for GPS data post-processing have been developed by different international research groups. In general, there are two GPS data post-processing approaches: relative positioning and absolute positioning. The advantages and disadvantages of these two post-processing approaches were discussed in previous publications (Grinter and Roberts 2011; Rizos et al. 2012; Wang 2013a).

The typical relative positioning approach uses the carrier-phase double-difference (DD) method, which fixes differenced phase ambiguities to integer values between stations and between satellites (Blewitt 1989; Dong and Bock 1989; Eckl et al. 2001; Herring et al. 2010). The DD method uses simultaneous observations from two or more GPS receivers; at least one of these receivers is in a known position with respect to a specific reference frame. The GAMIT/GLOBK software package developed and maintained by the Massachusetts Institute of Technology (MIT) is a typical post-processing package that implements the DD method (Herring et al. 2010). The GAMIT/GLOBK software package is freely available to the research community. There are several online post-processing services that also implement the DD method in their data processing, such as the Online Positioning User Service (OPUS, http://www.ngs.noaa.gov/OPUS/) operated by NGS at NOAA of USA and the online GPS processing service operated by the Geoscience Australia (AUSPOS, http://www.ga.gov.au). OPUS had been demonstrated as a reliable and precise post-processing approach for landslide surveying in the PRVI region (Wang 2013b; Wang and Soler 2012, 2014).

Precise point positioning (PPP) is a typical absolute positioning approach for GPS data processing. This method uses un-differenced dual-frequency pseudo-range and carrier-phase observations along with precise satellite orbit and clock information to determine the position of a stand-alone GPS station (Goad 1985; Zumberge et al. 1997; Kouba and Springer 2001; Ray et al. 2004; Kouba 2005). The absolute positioning approach solves for the position of a single GPS station without using any synchronous observations from other ground GPS stations, while using precise satellite ephemeris and clock information.

Several software packages that employ the PPP processing strategy have been developed, such as the GIPSY-OASIS software developed and maintained by JPL (https://gipsy-oasis.jpl.nasa.gov), the NRCan PPP software developed and maintained by the Natural Resources Canada (http://webapp.geod.nrcan.gc.ca/geod), the Bernese software developed and maintained by the Astronomical and the Physical Institutes of the University of Bern, Switzerland (http://www.bernese.unibe.ch), and the GAPS software developed and maintained by the University of New Brunswick (http://gaps.gge.unb.ca).

This article applied the single-receiver phase-ambiguity-fixed PPP method implemented in the JPL's GIPSY-OASIS software package (V6.3) (Bertiger et al. 2010). The PPP resolution applies the wide-lane and dual-frequency phase bias (WLPB) estimates for resolving the single-receiver phase ambiguity. The WLPB estimates are obtained from a global network of ground GPS stations. JPL's Final orbit clock and WLPB products are used in this study. The theoretical foundation of the PPP method is documented in Zumberge et al. (1997). The precision of the PPP solutions has been dramatically increased during the last decade. This is primarily attributed to highly precise satellite orbit and clock data provided by the International GNSS Service (IGS) (Dow et al. 2009), and new algorithms are used to resolve phase ambiguity with a single receiver (Bertiger et al. 2010). Other major parameters and key models applied in the PPP processing include the VMF1 troposphere mapping model (Boehm et al. 2006), second-order ionospheric delay (Kedar et al. 2003), ocean tidal loading model FES2004 (Lyard et al. 2006) calculated through the free online service operated by Onsala Space Observatory, Sweden (http://holt.oso.chalmers.se/loading), and tropospheric gradients (Bar-Sever et al. 1998; Lee et al. 2013; Morel et al. 2015).

The initial PPP solutions were in the loosely constrained frame of JPL's fiducial-free GPS orbits. They were transformed into the global reference frame IGb08 using daily 7-parameter transformations that are delivered with JPL's orbit products. IGb08 is a minor update of the IGS08 reference frame. The update is to restore a few of the IGS08 reference stations that had become unusable for operational reference frame alignments due to position discontinuities. IGb08 replaced IGS08 starting with products of GPS week 1709 (7 October 2012) (IGS Reference Frame Working Group 2012). The term IGb08 has not been widely used by GPS users outside the geodesy research community. Most publications associated with the applications of GPS still use the term IGS08 although their positions are referenced to IGb08 in the strict sense. For this reason, we use the term IGS08 rather than IGb08 in this article. The GIPSY processing and reference frame transformation were conducted within a geocentric Cartesian coordinate system (X, Y, Z). In order to track land surface deformation, the geocentric (X, Y, Z) coordinates were converted to cartographic coordinates (northing, easting, and ellipsoidal height) referred to the GRS-80 ellipsoid. An outlier detection and removing algorithm was applied to clean the positional or displacement time series in this study. On average, approximately 7 % of the total samples have been removed as outliers. The details of this approach were addressed in Firuzabadi and King (2011) and Wang (2011). According to our previous study and the results from this study (Table 3), the single-receiver phase-ambiguity-fixed PPP solutions (24-h average) are able to achieve 2–3 mm horizontal and 6–9 mm vertical precision (RMS) in the PRVI region.

1.3 PRVI reference frame of 2014 (PRVI14)

GPS data alone are not sufficient by itself to precisely delineate long-term ground deformation. In order to measure any change in the relative positions of sites on a dynamic

earth, a reference frame needs to be specified. The fact that GPS ground stations are located on moving lithospheric tectonic plates considerably complicates the reference frame issue.

In general, a global- or continental-scale reference frame is achieved with an approach of minimizing the overall horizontal movements of a large number of selected reference stations (DeMets et al. 2000, 2007; Larson et al. 1997; Altamimi et al. 2011; Wang et al. 2015). In the case of IGS08, 232 globally distributed and well-performing GPS stations were used (Rebischung et al. 2012). As a result, there are few "stable" (velocity equals zero) stations with respect to a global reference frame. The GPS stations in the PRVI region have a horizontal velocity of approximately 1.6 cm/year with respect to the global-scale reference frame IGS08 and 1.9 cm/year with respect to the regional-scale reference frame NAD83 (Fig. 3). NAD83 frame is a reference system that is relative to the fixed North American plate. It is mainly applied for land surveying and maintained by NGS (Snay and Soler 2000). It has been updated for several times, and the most recent realization is NAD83(2011) at epoch 2010.00. A reference frame covering a large area may be compromised by inter-plate as well as intra-plate motions. Slow ground deformation associated with local faulting and landslide creeping could be biased by plate motions. A preliminary local reference frame for the PRVI region was determined by Wang et al. (2014) with limited data (2009–2012). This study updated the previous reference frame with two additional years (2013 and 2014) of GPS observations and a better geographic configuration of reference stations.

The main physical and mathematical properties of a reference frame are the origin, the scale, the orientation, and the change of these parameters over time. In surveying and geodesy, a local reference frame is often tied to a well-established global reference frame with several common points. These common points are also called frame points or reference points. The velocities of these common points are minimized to zero over time with respect to the local reference frame. Such a local reference frame is also called a stable local reference frame, which is essential for precisely delineating long-term ground motions associated with landslide, subsidence, and faulting activities. In surveying and geodesy, the Helmert transformation method is often used to transform a set of points at a specific epoch from one reference frame into another one, within a three-dimensional space. For daily GPS positional coordinate transformation from the PPP solutions, the

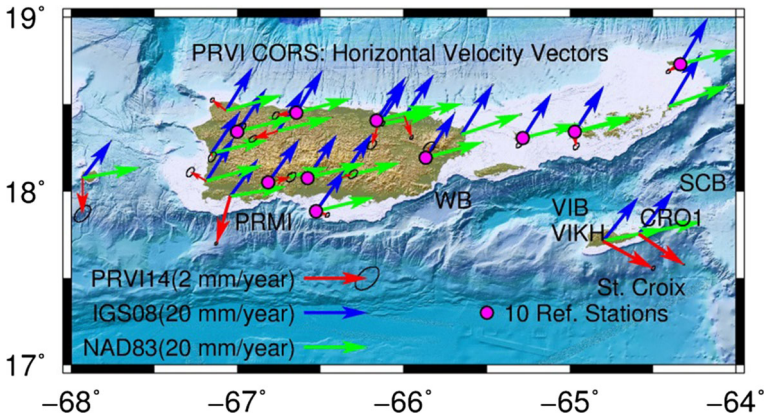

Fig. 3 Horizontal velocity vectors of CORS in the PRVI region with respect to three reference frames: a global reference frame (IGS08), a regional reference frame (NAD83), and a local reference frame (PRVI14)

geocentric coordinates of a site with respect to a local stable reference frame can be approximated by the following formulas (Snay 1999; Soler and Snay 2004; Pearson et al. 2010; Pearson and Snay 2013):

$$X(t)_{\text{Local}} = T_X(t) + [1 + s(t)] \cdot X(t)_{\text{IGS08}} + R_Z(t) \cdot Y(t)_{\text{IGS08}} - R_Y(t) \cdot Z(t)_{\text{IGS08}}$$

$$Y(t)_{\text{Local}} = T_Y(t) - R_Z(t) \cdot X(t)_{\text{IGS08}} + [1 + s(t)] \cdot Y(t)_{\text{IGS08}} + R_X(t) \cdot Z(t)_{\text{IGS08}}$$

$$Z(t)_{\text{Local}} = T_Z(t) + R_Y(t) \cdot X(t)_{\text{IGS08}} - R_X(t) \cdot Y(t)_{\text{IGS08}} + [1 + s(t)] \cdot Z(t)_{\text{IGS08}}.$$

Here, $T_X(t)$, $T_Y(t)$, and $T_Z(t)$ are translations at a specific epoch t along X-, Y-, and Z-axes; $R_X(t)$, $R_Y(t)$, and $R_Z(t)$ are counterclockwise rotations about these three axes; $s(t)$ is a differential scale change between IGS08 and the local reference frame. In practice, there

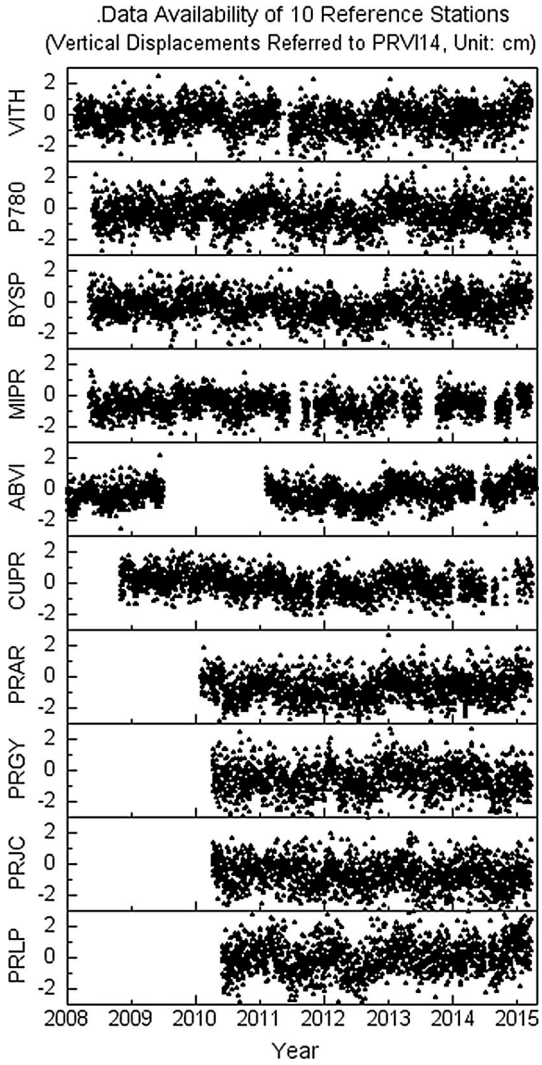

Fig. 4 *Plots* showing the data availability of ten reference stations for realizing the stable Puerto Rico and Virgin Islands reference frame of 2014 (PRVI14). Each *subplot* depicts the vertical positional time series of each reference station with respect to the PRVI14

are two approaches to perform the Helmert transformation: daily 7-parameter transformation and 14-parameter similarity transformation. For the 7-parameter method, the 7 parameters ($T_X(t)$, $T_Y(t)$, $T_Z(t)$, $R_X(t)$, $R_Y(t)$, $R_Z(t)$, and $s(t)$) for each epoch (day) are calculated from the positional coordinates (X, Y, Z) of these reference stations with respect to both source and target reference frames at the same day. For the 14-parameter transformation, these 7 parameters for each day are calculated by a linear regression method, which can be written as:

$$H(t) = H(t_0) + H' \cdot (t - t_0).$$

Here, $H(t)$ represents the seven Helmert transformation parameters at a specific epoch; t_0 denotes an initial epoch (e.g., 2013.0); H' represents the rate of the change of each parameter over time. In practice, H' is regarded as a constant that can be obtained from the Helmert parameters on two selected epochs t_2 and t_1:

$$H' = \frac{H(t_2) - H(t_1)}{t_2 - t_1}.$$

In this study, t_2 and t_1 are set as 2015.0 and 2009.0, respectively. The detailed method for calculating the 14 parameters is addressed in Wang et al. (2013b, 2014).

The selection of reference stations is critical for establishing a precise local reference frame. In general, the selection is primarily based on data availability (e.g., >5 years), site stability, and overall geographic distribution. It is difficult to determine the stability of a GPS site at the level below 1 mm/year prior to having a precise stable local reference frame. Accordingly, a trial-and-error approach is used in this study to refine the selection of reference stations. Initially, fifteen stations with a history over 5 years were selected as reference stations, and the 14 parameters for reference frame transformation were calculated. It turned out that three stations (PRMI, CRO1, and VIKH) had considerably larger horizontal velocities than the other twelve stations with respect to the initial local reference frame. These three stations were removed from the selected reference stations, and the 14 parameters were recalculated. Any station that had a horizontal velocity larger than 0.5 mm/year with respect

Table 2 Fourteen parameters for Helmert reference frame transformation from IGS08 to PRVI14

Parameters	Unit	IGS08 to PRVI14 $t_0 = 2013.0$
$T_x(t_0)$	m	0.0
$T_y(t_0)$	m	0.0
$T_z(t_0)$	m	0.0
$R_x(t_0)$	radian	0.0
$R_y(t_0)$	radian	0.0
$R_z(t_0)$	radian	0.0
$s(t_0)$	unitless	0.0
dT_x	m/year	4.77E−3
dT_y	m/year	1.07E−2
dT_z	m/year	2.68E−02
dR_x*	radian/year	−3.95E−09
dR_y*	radian/year	−7.14E−09
dR_z*	radian/year	4.54E−09
ds	1/year	0.0

* Counterclockwise rotations of axes (X, Y, Z) are positive

to the resulted local reference frame was removed from the group of reference stations, and the 14 parameters were recalculated again. Finally, ten CORS were selected as reference stations after several trials and considering the overall geographic distribution. All reference stations have continuous observations for at least 5 years. The locations and data availability of these ten reference stations are illustrated in Table 3 and Fig. 4. The average three-component velocities of these ten reference stations with respect to the PRVI14 are 0.4 mm/year in the east–west (EW), 0.2 mm/year in the north–south (NS), and 0.5 mm/year in the vertical components (Table 3). The 14 parameters for the updated PRVI reference frame

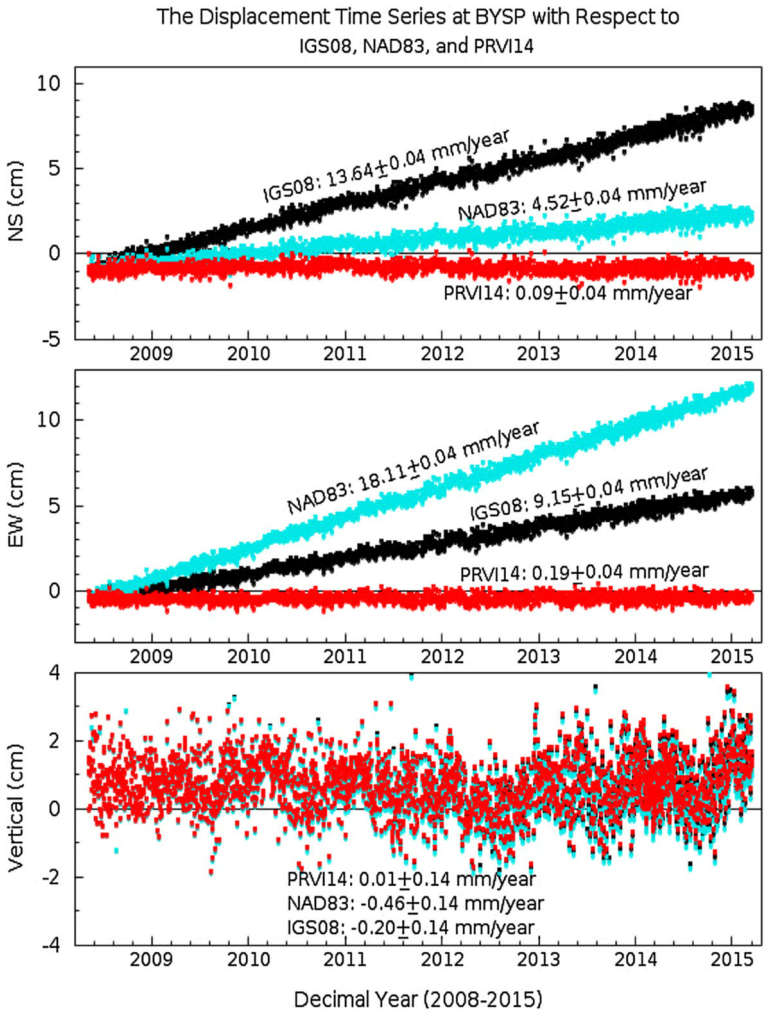

Fig. 5 Geodetic displacement time series at BYSP with respect to three different reference frames: a global reference frame (IGS08), a regional reference frame (NAD83), and a local reference frame (PRVI14). The linear velocity (v) and its corresponding two times "standard error" (2σ) for each displacement time series are marked aside. Statistically, "$v \pm 2\sigma$" indicates that there is a 95 % possibility that the true velocity would be within the interval between $v - 2\sigma$ and $v + 2\sigma$, assuming that the uncertainty (*error*) fits normally distributed white noise

(PRVI14) are listed in Table 2. The horizontal velocity vectors of all CORS in the PRVI region with respect to PRVI14 are plotted in Fig. 3.

Figure 5 depicts the long-term displacement time series at BYSP with respect to three reference frames with different scales: a global reference frame (IGS08), a regional reference frame (NAD83), and a local reference frame (PRVI14). It is clear that BYSP is stable with respect to the local reference frame (PRVI14, 0.2 mm/year in horizontal plane) while keeps moving with respect to both the global (IGS08, 1.6 cm/year in horizontal plane) and regional (NAD83, 1.9 cm/year in the horizontal plane) reference frames. We use "standard error" to assess the precision (uncertainty) of the linear regression in this study. The standard error (σ) is the standard deviation of the sampling distribution of a statistic, mostly the mean or the root-mean-square (RMS). For the linear velocity regression analysis conducted in this study, the term "standard error" indicates standard deviation of the underlying errors (uncertainties) of the estimated linear velocity. The linear velocity (v) and its corresponding two times "standard error" (2σ) for each displacement time series are marked on each subplot. Statistically, "$v \pm 2\sigma$" indicates that there is a 95 % possibility that the true velocity would be within the interval between $v - 2\sigma$ and $v + 2\sigma$, assuming the error fits normally distributed white noise. The precision (2σ) of the horizontal velocity estimations with respect to all three reference frames is 0.04 mm/year. The 14-parameter transformation processing did not improve the precision of velocity estimates since a linear regression model was applied to the changes of the scale, three translational, and three rotational motions in time. A linear model employed in the frame transformation would remove certain common linear movements but not periodical seasonal motions. In contrast, a daily 7-parameter reference transformation processing may improve the precision of velocity estimates because certain localized common motions (mostly seasonal motions) would be removed during the transformation (Blewitt et al. 2013; Rebischung et al. 2012; Altamimi et al. 2011). The difference between the 14-parameter and daily 7-parameter reference frame transformation approaches implies that the

Table 3 Velocities and repeatability (RMS) of the PPP solutions of ten reference stations with respect to PRVI14

Stations	Geodetic coordinates			Site velocity			Repeatability of PPP solutions		
	Longitude (°)	Latitude (°)	Ellip. height (m)	NS (mm/year)	EW (mm/year)	UD (mm/year)	NS (mm)	EW (mm)	UD (mm)
PRJC	−66.9995	18.34223	22.8537956	0.1	0.1	−0.8	2.7	2.8	8.9
PRGY	−66.81443	18.05095	18.05095177	0.2	0.7	0.0	2.9	2.8	9.4
P780	−66.57913	18.07503	18.07502617	0.1	0.0	−0.1	2.6	2.4	8.7
PRAR	−66.64742	18.45048	18.45047792	−0.1	−0.6	0.6	2.5	2.2	8.2
MIPR	−66.52696	17.88622	17.88622395	−0.1	0.4	−0.1	1.9	1.9	6.6
BYSP	−66.1612	18.40784	18.40783715	−0.1	0.2	0.0	2.4	2.1	7.7
PRLP	−65.86826	18.1949	18.19490096	0.3	0.1	1.0	2.7	2.8	9.3
CUPR	−65.28252	18.30744	13.30743945	−0.2	−0.1	−0.9	2.3	2.2	6.8
VITH	−64.96921	18.34333	18.34333171	0.1	0.0	0.0	3.1	2,3	8.1
ABVI	−64.33248	18.72968	16.26230587	−0.2	−0.4	0.2	2.0	1.9	6.1
Average (RMS)				0.2	0.4	0.5	2.5	2.4	8.1

14-parameter approach would be a better choice for studies focusing on regional seasonal or other periodical motions.

1.4 Neotectonic faulting

Numerous bedrock faults have been mapped in Puerto Rico, most notably the Great Southern Puerto Rico fault zone and the Great Northern Puerto Rico fault zone, as well as smaller faults such as the Cerro Goden, Punta Algarrobo near Mayaguez, Punta Guanajibo faults, and South Lajas fault (DeMets et al. 2000; Jansma et al. 2000; Mann et al. 2002; Jansma and Mattioli 2005; Prentice and Mann 2005). Figure 3 indicates that only three GPS stations (PRMI, VIKH and CRO1) show considerable (>1 mm/year) horizontal movements with respect to the PRVI14. All other stations are almost stable (<0.5 mm/year) with respect to the PRVI14. The average horizontal velocity of these ten reference stations with respect to the PRVI14 is about 0.4 mm/year (Table 3), which implies that the rigidity of the Puerto Rico Island is at the level of approximately 0.4 mm/year.

Figure 6 illustrates the three-component displacement time series at PRMI and CRO1. PRMI is located on the Magueyes Island, a small island (about 0.07 km^2) 2 km south to the southern boundary of the Lajas Valley. CRO1 is located on the St. Croix Island, which is geographically a part of the Virgin Islands (VI). The horizontal components of PRMI depict a horizontal velocity vector of 1.6 mm/year toward the southwest, which might be associated with the neotectonic faulting within the Lajas Valley in the southwestern Puerto Rico (Fig. 7). The Lajas Valley is an east–west trending depression zone, 30 km long bounded by hills on its northern and southern edges. This area has the most frequent

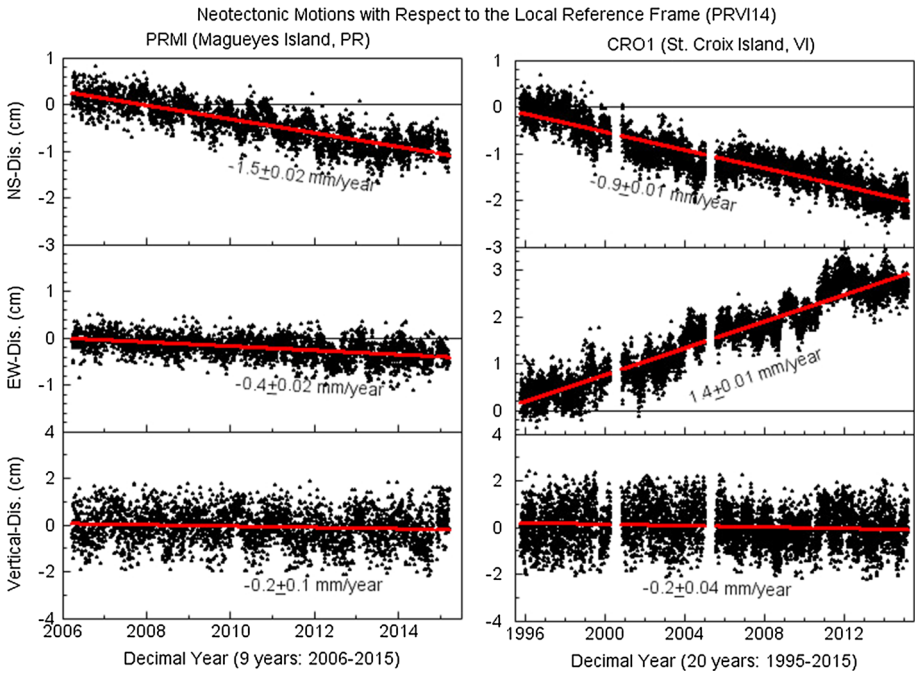

Fig. 6 Three-component displacement time series at PRMI and CRO1. *Both sites* indicate steady horizontal movements that associated with current neotectonic motions (or strain accumulation)

onshore microseismicity in the PRVI region (Asencio 1980). Previous researchers have recognized possible Quaternary fault control for the Lajas Valley on the basis of geomorphology (Joyce et al. 1987) and seismic reflection profiles (Meltzer and Almy 2000). Displacements along the EW-striking faults were inferred to be normal with a component of strike slip (Meltzer 1997; Almy et al. 2000; Prentice et al. 2000). Prentice and Mann (2005) excavated a trench across a scarp near the southern edge of the Lajas Valley that exposed a narrow fault zone disrupting alluvial deposits. Trenching across the fault scarp showed that the South Lajas fault is an active Holocene structure, with movement within the past 5000 years. Huérfano et al. (2005) established left-lateral stress pattern in Lajas Valley and northeast-southwest extension within the southwest coast region of Puerto Rico on the basis of the microseismic activity analysis. Roig-Silva et al. (2013) proposed a major through-going left-lateral strike-slip fault zone that cuts across the Lajas Valley. ten Brink and Lopez-Venegas (2012) stated that the PRMI station was moving to the southwest at a rate of 2.3 mm/year relative to the Caribbean plate and suggested a boundary between Hispaniola and the PRVI region that lied north of PRMI. GPS measurements presented in this study indicated that PRMI is moving to the southwest with respect to the PRVI14 reference frame. This implies the occurrence of northeast-southwest extension in the southwest Puerto Rico. The extension may suggest that the Lajas Valley currently experiences a north–south direction extension (1.5 mm/year) and minor right-lateral strike slip (Fig. 7). The current GPS geodetic infrastructure in the PRVI region provides a higher precision for neotectonic faulting study than the limited geodetic resource of a decade ago (DeMets et al. 2000; Jansma et al. 2000; Mann et al. 2002; Jansma and Mattioli 2005).

The two CORS (CRO1 and VIKH) on the St. Croix Island show identical velocity vectors of 1.7 mm/year toward southeast with respect to the PRVI14 (Fig. 3). The antenna of VIKH is mounted on the side wall of a one-floor concrete building. The antenna of CRO1 is mounted on a concrete monolith that was poured to a depth of 3.5 m and extended 0.64 m above the ground surface (personal communication with Mr. David Stowers at the Jet Propulsion Laboratory, 2015). CRO1 has a history of 20 years (1995–2015). VIKH has a history of 9 years (2006–2015). The consistent velocity vectors from these two stations suggest the ongoing extension of the Virgin Islands basin, which is consistent with the result presented by Jansma and Mattioli (2005). The Virgin Islands basin has a rhomboidal

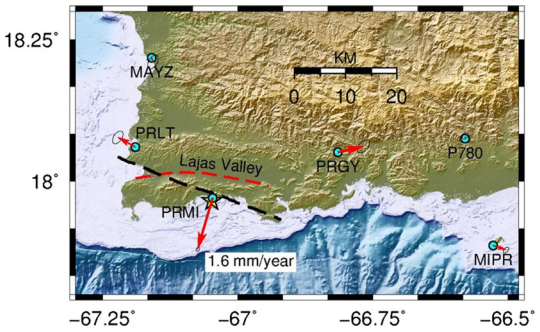

Fig. 7 GPS derived horizontal velocity vectors (*red arrow*) showing the possible extension of the Lajas Valley. The CORS (*cyan circle*) PRMI is proximal (0.5 km apart) to a long-history tide gauge station (*yellow star*). The *red dashed line* represents the South Lajas Fault presented in Prentice and Mann (2005). The *black dashed line* represents the North Boqueron Bay-Punta Montalva Fault Zone presented in Roig-Silva et al. (2014)

shape with a long axis of about 80 km in a nearly east–west (EW) direction and a short axis of about 20 km in a nearly north–south (NS) direction. This basin has a complex bathymetry with the deepest water reaching a depth of over 4500 m below sea level. Recent seismic activities demonstrate that the Virgin Islands basin area is tectonically active (Reid and Taber 1920; Frankel et al. 1980; ten Brink et al. 2011; Liu and Wang 2015). Previous investigations based on high-resolution bathymetry data, seismic survey data, and geologic study suggest that the sedimentary structure within the Virgin Islands basin is characterized by a complex system of strike-slip faults (Raussen et al. 2013). Barkan and ten Brink (2010) stated that the seismic reflection profiles across the Virgin Islands basin have an asymmetric sediment fill, which thickens to the south. This result implies that the Virgin Islands basin is a half graben structure and its southern boundary of the basin could have been more active than the northern boundary throughout the geologic history. The 1867 Virgin Islands earthquake (M7.5) occurred in this basin (McCann 1985; Barkan and ten Brink 2010). The main shock generated a tsunami with waves that were recorded at several island locations across the eastern region of the Caribbean, most notably on the islands of St. Thomas and St. Croix (Reid and Taber 1920). Previous investigators proposed different tectonic mechanisms to explain the origin of the basin and the present faulting motions within the basin. Three controversial faulting motions have been suggested: (1) left-lateral (Hess and Maxwell 1953; Donnelly 1964; Mann and Burke 1984; Lithgow et al. 1987; Gill et al. 1999; ten Brink 2005; Raussen et al. 2013), (2) right-lateral (Nemec 1980; Matthews and Holcombe 1976; Jany et al. 1990; Masson and Scanlon 1991; Loureiro 2014), and (3) northwest-southeast direction opening across the basin (Murphy and McCann 1979; Speed and Larue 1991; Feuillet 2002; Mann et al. 2005). GPS velocity vectors obtained from this study suggest that the current neotectonic motions (or strain accumulation) within the basin are comprised of two components: an extension (0.9 mm/year) along the north–south direction and a left-lateral strike slip (1.4 mm/year) along the east–west direction with respect to the PRVI14 (Fig. 6). The quantitative results from the long-term GPS measurements provide critical information for assessing the present seismic risk in the PRVI region.

The vertical displacement time series at PRMI and CRO1 show a steady 0.2 mm/year subsidence rate with respect to the PRVI14, which falls below the precision limit (0.5 mm/year) that can be distinguished by the current local reference frame (PRVI14). For this reason, we do not intend to interpret vertical motions in this article.

1.5 Landslide monitoring

Mountainous terrain and a tropical climate make the PRVI region highly susceptible to landslide hazards. One of the most catastrophic landslides in the USA occurred in Mameyes, south of Puerto Rico in October 1985 (Silva-Tulla 1986). The death toll that resulted from the Mameyes landslide was over 100 people. This was the worst loss of life that resulted from a single landslide in US history (Jibson 1986, 1989). Long-term continuous monitoring of ground movements is essential for identifying suspected landslides, predicting the behavior of active landslides, and assessing the potential for landslide hazards. GPS technologies have been frequently applied for the purpose of landslide monitoring worldwide. GPS landslide monitoring projects have conventionally been carried out using the differential positioning method. This method could achieve sub-centimeter accurate result if the baseline is short (e.g., <50 km). The authors conducted GPS monitoring on several landslides in Puerto Rico during the period from 2009 to 2011 (Wang et al. 2011; Wang 2012; Wang et al. 2013a). In order to monitor a sliding mass, at

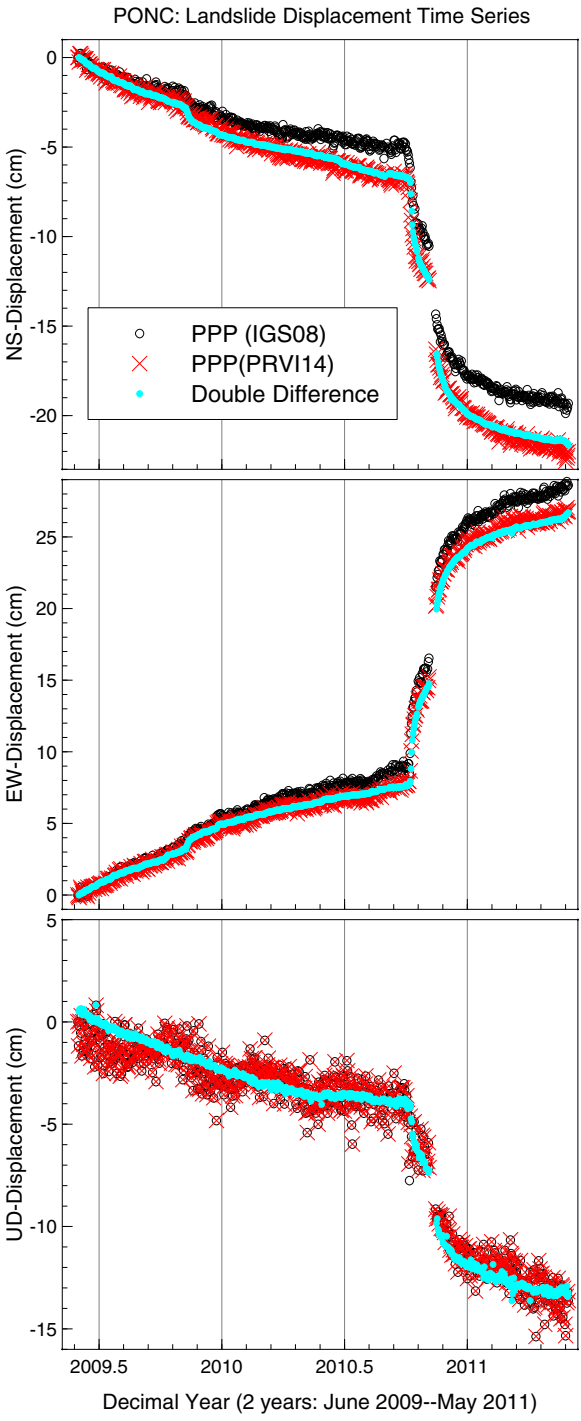

Fig. 8 *Plots* showing the application of the local reference frame (PRVI14) in landslide monitoring. Using a global reference frame will underestimate the long-term displacement in the NS direction and overestimate the long-term displacement in the EW direction

least one reference station had to be installed outside of the suspected sliding mass. The rover data could not be processed without simultaneous data from the reference station. It happened for several times that the field efforts were ruined by unrealized power or cable connection problems at the reference station.

This study established the stable local reference frame based on the 6 years of data accumulation (2009–2014) in the PRVI region. Precise landslide monitoring can be conducted with the local reference frame and without specific reference stations in the field. Figure 8 illustrates the three-component displacement time series derived from GPS observations at a landslide site in Ponce, Puerto Rico. This landslide has been carefully investigated in our previous publications (Wang 2012; Wang and Soler 2012). We reprocessed the landslide data with the PPP method and transformed the displacement time series (IGS08) to the local reference frame (PRVI14). The cyan points shown in Fig. 8 represent solutions from the differential method that used one rover station and one reference station in the field. The baseline between the reference station and the rover station was 113 m. The short baseline resulted in extremely high precision (repeatability) of the double-differencing (DD) solutions. According to our previous study, the DD solutions achieved 0.3 mm horizontal precision and 0.9 mm vertical precision (RMS) (Wang 2012). The red crosses shown in Fig. 8 represent the PPP solutions with respect to the PRVI14. The comparison indicates that the two methods resulted in the same interpretation on the kinematics of the landslide although the differential method resulted in a higher precision. The PPP processing and the local reference frame (PRV14) combined method demonstrates a more efficient approach of conducting landslide surveying than the conventional DD method. No reference stations are needed for conducting millimeter-level landslide monitoring in the PRVI region from now on.

1.6 Absolute sea-level monitoring

The National Ocean Service of NOAA and the Puerto Rico Seismic Network (PRSN) operate a real-time sea-level monitoring system that comprises 16 tide gauge stations along the coasts of Puerto Rico and the US Virgin Islands (see Fig. 1). A tide gauge is commonly used to measure sea level in coastal areas. Sea level measured by a tide gauge is the height relative to the level of a geodetic benchmark on the nearby land, so vertical motion of land will cause a relative sea-level change. This makes it impossible to distinguish whether the water is rising or the land is subsiding from the tide gauge measurements alone. All tide gauge sites in the PRVI region are co-located or proximal (<5 km) to at least one CORS. The absolute ground altitude change can be measured by GPS, and then, the absolute sea-level change can be calculated from the tide gauge measurements. The PRSN is in the process of integrating the real-time GPS and tide gauge data into its tsunami warning program. A tsunami early-warning system consists of two important components: tsunami early-warning and tsunami verification following a tsunami warning. The early-warning system is primarily based on real-time seismic observations to identify tsunamigenic earthquakes. The tsunami verification system is based on real-time absolute sea-level measurements from the tide gauge system. It is critical to verify or cancel the predicted tsunamis based on the observed absolute sea-level observations. Gradually more GPS instruments will be added to the existing tide gauge sites in the Caribbean region, and the co-located GPS and tide gauge system is expected to provide absolute sea-level measurements in real-time (Braun et al. 2012; Feaux et al. 2012; Mattioli et al. 2012). The NOAA Tsunami Warning Centers and the PRSN are exploring ways to operationally integrate GPS observations into the early-warning system.

The GPS and tide gauge integrated system is also significant for delineating long-term sea-level changes. A significant proportion of the global population, including those in many of the world's large cities, are located close to coastal areas. This section illustrates the potential application of the PRVI GPS geodetic infrastructure in long-term sea-level rise monitoring. Figure 9 illustrates the relative sea-level measurements from two tide gauge stations in the PRVI region. The tide gauge on the Magueyes Island has a continuous recording history of 60 years (1955–2015). It is approximately 0.5 km apart from the CORS PRMI (2006–2015). The tide gauge on the St. Croix Island has a continuous recording history of 38 years (1977–2015), which is approximately 3.5 km to the CORS VIKH (2006–2015) and 19 km to the CORS CRO1(1995–2015). The monthly sea-level data are obtained from the Permanent Service for Mean Sea Level (PSMSL, http://www.psmsl.org) (Holgate et al. 2013), a public sea-level data archiving facility based in Liverpool at the National Oceanography Centre (NOC) of the UK Natural Environment Research Council (NERC).

The relative sea-level measurements were decomposed to three components: nonlinear trend, seasonal, and remainder (Fig. 9). The Seasonal Trend Decomposition using Loess (STL) program was applied to extract seasonal information from the original sea-level data. The STL is a filtering procedure employing a locally weighted regression (Loess) for decomposing a time series into nonlinear trend, seasonal, and remainder components

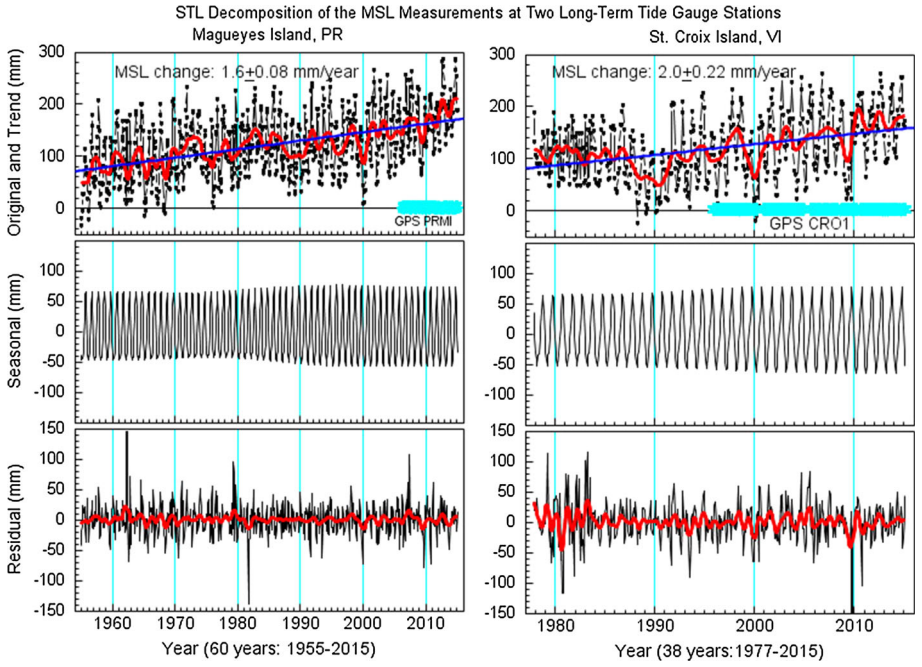

Fig. 9 *Plots* showing STL decompositional sea-level measurements from two tide gauge stations on the Magueyes Island (*left*) of Puerto Rico and the Lime Tree Bay of St. Croix Island (*right*). The *top subplots* depict original sea-level measurements (*dark*), the nonlinear trend (*red*) obtained from the seasonal signals removed sea-level measurements, average seal-level change rate (*blue*) obtained by applying a linear regression model to the nonlinear trend, and closely spaced GPS vertical measurements (*cyan*). The *middle subplots* show the seasonal signals. The *bottom subplots* show the residual after removing the nonlinear trend and the seasonal signals

(Cleveland et al. 1990). Loess is a method for estimating nonlinear relationships (Cleveland and Grosse 1990; Cleveland and Devlin 1988). STL is a very versatile and robust method for decomposing time series. The average sea-level change rate was obtained by applying a linear regression model on the nonlinear trend component, the red line in the top row of Fig. 9. The tide gauge measurements indicate an average relative sea-level rise of 1.6 ± 0.08 mm/year in the Magueyes Island coastal area and an average relative sea-level rise of 2.0 ± 0.22 mm/year in the St. Croix Island coastal area with respect to the ground surface at each tide gauge site. Long-term continuous measurements from the two GPS stations indicate that there are no considerable vertical ground motions (-0.2 ± 0.1 mm/year in PRMI, -0.2 ± 0.04 mm/year in CRO1) at both the tide gauge sites though both GPS sites experience steady horizontal motions (Fig. 6). Thus, the average sea-level rise rates obtained from the tide gauges represent the absolute sea-level rise rates.

2 Discussion and conclusions

This article summarized the current GPS geodetic infrastructure in the PRVI region, which is comprised of three fundamental components: (1) the CORS network that is operated and maintained by the joint efforts of the PRSN, the private land surveying company HLCM Group Inc., UNAVCO, NGS, Coastal Guard, FAA, JPL, and other agencies; (2) the stable local reference frame (PRVI14) that will be incrementally improved and periodically updated to synchronize with the update of the IGS reference frame; and (3) the sophisticated GPS data processing software packages (e.g., GIPSY, GAMIT) that are freely available to the research community. The primary product from present study is the stable Puerto Rico and Virgin Islands reference frame (PRVI14), specifically the 14 Helmert transformation parameters for converting coordinates from IGS08 to the stable local reference frame (PRVI14) (Table 2). The PRVI14 provides a consistent and stable reference with which geometric results can be produced and compared over space and time. The local geodetic infrastructure provides a platform for multiple natural hazards studies. This study illustrates its initial application in neotectonics, landslide, and sea-level studies. A better understanding of neotectonics in the PRVI region will improve regional seismic hazard assessment. The geodetic infrastructure will also be useful for hydrologists to study ground deformations from fluid withdrawal, aquifer deformation, seasonal hydrologic and atmospheric pressure loading, for geomorphologists to study coastal erosion and wetland loss problems along the PRVI coasts, and for engineers to monitor long-term stabilities of local dams, sea walls, high-rise buildings, and long-span bridges.

The precision of GPS has continuously improved during the past two decades. From this investigation, the single-receiver phase-ambiguity-fixed PPP daily solutions are able to provide 2–3 mm repeatability for horizontal and 6–9 mm repeatability for vertical measurements in the PRVI region. The local reference frame (PRVI14) will be able to identify ground movement as slow as 0.4 mm/year and 0.5 mm/year in horizontal and vertical directions within a period as short as 5 years, respectively. The way to process GPS data in the office directly impacts the way to collect data in the field. The combination of the PPP processing and the local reference frame provides an efficient way of conducting ground deformation monitoring with a stand-alone GPS unit in the field without installing any reference stations.

In this study, the realization of IGS08 solutions was performed on a local computer installed with the GIPSY/OASIS (V6.3) software. Fortunately, several free online PPP

services are also available to the geodesy research and application communities, such as the Automatic Precise Positioning Service provided by the JPL (APPS, http://apps.gdgps.net/apps_file_upload.php) and the CSRS-PPP Online Service provided by the Natural Resources Canada (http://webapp.geod.nrcan.gc.ca/geod/tools-outils/ppp.php?locale=en). Occasional users may conveniently upload their GPS data (RINEX files) manually through the Web site of APPS or CSRS-PPP. Positions with respect to the IGS08 reference frame are available in minutes by e-mail. The global positions can be transformed to PRVI14 by using the 14 parameters and formulas provided in this article. Thus, a technician with basic GPS and computing knowledge will be able to conduct millimeter-level ground deformation monitoring using a stand-alone GPS unit. This approach would significantly reduce costs and logistics for natural hazards monitoring and surveying. Therefore, it is an attractive alternative to the conventional survey techniques. A great number of CORS have been installed worldwide during the past decades, which have accumulated fundamental data for establishing stable local reference frames in different regions. It is hoped that this study will promote the applications of the GPS techniques in natural hazards research and mitigation in the PRVI region and other natural hazard-prone areas.

Acknowledgments This PRSN GPS network was funded by the NSF award EAR-0722540 and the NOAA award DG133W13CN0023. This study was supported by the NSF CAREER award EAR-1229278, NSF TUES award DUE-1243582 and the NSF "COCONET" award EAR-1042906. The authors appreciate the efforts from UNAVCO and NGS for archiving GPS data for the geodesy community. The authors thank Dr. Glen Mattioli at UNAVCO, Dr. Yan Jiang at the Geological Survey of Canada, one anonymous reviewer and the editor for their comments and thoughtful suggestions.

References

Almy C, Meltzer A, Dietrich C (2000) Faulting in the Lajas Valley and on the adjacent shelf. southern Puerto Rico: EOS (Transactions, American Geophysical Union), **F1181**

Altamimi Z, Collilieux X, Métivier L (2011) ITRF2008: an improved solution of the international terrestrial reference frame. J Geodesy 85:457–473. doi:10.1007/s00190-011-0444-4

Aponte J, Meng X, Hill C, Moore T, Burbidge M, Dodson A (2009) Quality assessment of a network-based RTK GPS service in the UK. J Appl Geodesy 3:25–34

Asencio E (1980) Western Puerto Rico Seismicity. USGS Open File Report: 80–192

Barkan R, ten Brink US (2010) Tsunami simulations of the 1867 Virgin Island earthquake: constraints on epicenter location and fault parameters. Bull Seismol Soc Am 100:995–1009. doi:10.1785/0120090211

Bar-Sever YE, Kroger PM, Borjesson JA (1998) Estimating horizontal gradients of tropospheric path delay with a single GPS receiver. J Geophys Res Solid Earth 103:5019–5035. doi:10.1029/97JB03534

Benford B, DeMets C, Calais E (2012) GPS estimates of microplate motions, northern Caribbean: evidence for a Hispaniola microplate and implications for earthquake hazard. Geophys J Int 191(2):481–490. doi:10.1111/j.1365-246X.2012.05662.x

Bertiger W, Desai SD, Haines B, Harvey N, Moore AW, Owen S, Weiss JP (2010) Single receiver phase ambiguity resolution with GPS data. J Geodesy 84:327–337. doi:10.1007/s00190-010-0371-9

Blewitt G (1989) Carrier phase ambiguity resolution for the Global Positioning System applied to geodetic baselines up to 2000 km. J Geophys Res 94(B8):10187–10203

Blewitt G, Kreemer C, Hammond WC, Goldfarb JM (2013) Terrestrial reference frame NA12 for crustal deformation studies in North America. J Geodyn 72:11–24

Boehm J, Niell A, Tregoning P, Schuh H (2006) Global mapping function (GMF): a new empirical mapping function based on numerical weather model data. Geophys Res Lett. doi:10.1029/2005GL025546

Braun JJ, Calais E, Dausz K, Feaux K, Friesen B, Mattioli G, Miller MM, Normandeau J, Seider E, Wang G (2012) COCOnet (Continuously Operating Caribbean GPS Observational Network): infrastructure enhancements to improve sea level monitoring. Geol Soc Am 44(7):229

Calais E, Mazabraud Y, Mercier de Lepinay B, Mann P, Mattioli G, Jansma P (2002) Strain partitioning and fault slip rates in the northeastern Caribbean from GPS measurements. Geophys Res Lett 29:1856. doi:10.1029/2002GL015397

Cleveland WS, Devlin SJ (1988) Locally-weighted regression: an approach to regression analysis by local fitting. J Amer Statist As 83:596–610
Cleveland WS, Grosse E (1990) Fitting curves and surfaces to data. Wadsworth Advanced Books and Software, Monterey
Cleveland RB, Cleveland WS, McRae JE, Terpenning I (1990) STL: a seasonal-trend decomposition procedure based on loess. J Off Stat 6:3–73
Clinton JF, Cua G, Huérfano CV, von Hillerbrandt-Andrade CG, Martínez-Cruzado J (2006) The current state of seismic monitoring in Puerto Rico. Seismo Res Lett 77(5):5–12
DeMets C, Jansma PE, Mattioli GS, Dixon TH, Farina F, Bilham R, Calais E, Mann P (2000) GPS geodetic constraints on Caribbean-North America plate motion. Geophys Res Lett. doi:10.1029/1999GL005436
DeMets C, Mattioli GS, Jansma P, Rogers R, Tenorios C, Turner HL (2007) Present motion and deformation of the Caribbean plate: constraints from new GPS geodetic measurements from Honduras and Nicaragua. In: Mann P (ed) Geologic and tectonic development of the Caribbean Plate in Northern Central America. Geol Soc Am Spec Pap 428:21–36. doi:10.1130/2007.2428(02)
Dixon TH, Gonzalez G, Lichten SM, Katsigris E (1991) First epoch geodetic measurements with the Global Positioning System across the northern Caribbean plate boundary zone. J Geophys Res 96:2397. doi:10.1029/90JB02003
Dixon TH, Farina F, DeMets C, Jansma P, Mann P, Calais E (1998) Relative motion between the Caribbean and North American plates and related boundary zone deformation from a decade of GPS observations. J Geophys Res 103:15157. doi:10.1029/97JB03575
Dong D, Bock Y (1989) Global Positioning System network analysis with phase ambiguity resolution applied to crustal deformation studies in California. J Geophys Res 94(B4):3949–3966. doi:10.1029/JB094iB04p03949
Donnelly TW (1964) Evolution of eastern Greater Antillean island arc. Am As Pet Geol Bull 48:680–696. doi:10.1306/BC743D23-16BE-11D7-8645000102C1865D
Dow JM, Neilan RE, Rizos C (2009) The international GNSS service in a changing landscape of Global Navigation Satellite Systems. J Geodesy 83:191–198
Eckl MC, Snay RA, Soler T, Cline MW, Mader GL (2001) Accuracy of GPS-derived relative positions as a function of interstation distance and observing-session duration. J Geodesy 75(12):633–640
Feaux K, Braun JJ, Calais E, Dausz K, Friesen BT, Mattioli GS, Miller MM, Normandeau J, Seider E, Wang G (2012) COCONet (Continuously Operating Caribbean GPS Observational Network): network status and project highlights. AGU Fall meeting Abstract #T41A-2556, San Francisco, California
Feuillet N (2002) Arc parallel extension and localization of volcanic complexes in Guadeloupe, Lesser Antilles. J Geophys Res 107:1–29. doi:10.1029/2001JB000308
Firuzabadi D, King RW (2011) GPS precision as a function of session duration and reference frame using multi-point software. GPS Solut 16:191–196. doi:10.1007/s10291-011-0218-8
Frankel A, McCann WR, Murphy AJ (1980) Observations from a seismic network in the Virgin Islands region: tectonic structures and earthquake swarms. J Geophys Res 85:2669–2678. doi:10.1029/JB085iB05p02669
Gill I, Mclaughlin PP, Hubbard DK (1999) Evolution of the neogene kingshill basin of St. Croix, U.S. Virgin Islands. In: Mann P (ed) Sendimentary basins of the world, vol. 4. Caribbean Basins, Elsevier Science, Amsterdam, pp 343–366. doi:10.1016/S1874-5997(99)80047-1
Goad C (1985) Precise relative positioning determination using Global Positioning System carrier phase measurements in a nondifferenced mode. In: Proceedings of the 1st international symposium on Precise Positioning System with the Global Positioning System, US Department of Commerce, National Oceanic and Atmospheric Administration, Silver Spring, MD: 347–356
Grinter T, Roberts C (2011) Precise point positioning: Where are we now? In: Proceedings of the IGNSS symposium (IGNSS2011), Sydney, Australia, 2011. http://www.lpi.nsw.gov.au/__data/assets/pdf_file/0020/165701/2011_Grinter_and_Roberts_IGNSS2011_PPP_where_are_we_now.pdf. Accessed 22 Jan 2016
Herring TA, King RW, McCluskey SC (2010) Introduction to GAMIT/GLOBK, release 10.4. Massachusetts Institute of Technology, Cambridge. http://www-gpsg.mit.edu/~simon/gtgk/down.htm. Accessed 17 June 2015
Hess HH, Maxwell JC (1953) Caribbean research project. Bull Geol Soc Am 64:1–6. doi:10.1130/0016-7606(1953)64
Holgate SJ, Matthews A, Woodworth PL, Rickards LJ, Tamisiea ME, Bradshaw E, Foden PR, Gordon KM, Jevrejeva S, Pugh J (2013) New data systems and products at the permanent service for mean sea level. J Coast Res 29(3):493–504. doi:10.2112/JCOASTRES-D-12-00175.1
Huérfano V, von Hillebrandt-Andrade CG, Báez-Sanchez G (2005) Microseismic activity reveals two stress regimes in southwestern Puerto Rico. Geol Soc Am Spec Pap 385:81–101

IGS Reference Frame Working Group (2012) IGb08: an update on IGS08. https://igscb.jpl.nasa.gov/pipermail/igsmail/2012/007853.html. Accessed 22 Jan 2016

Jansma PE, Mattioli GS (2005) GPS results from Puerto Rico and the Virgin Islands: constraint on tectonic setting and rates of active faulting. Geol Soc Am Spec Paper 385:13–30. doi:10.1130/0-8137-2385-X.13

Jansma PE, Mattioli GS, Lopez A, DeMets C, Dixon TH, Mann P, Calais E (2000) Neotectonics of Puerto Rico and the Virgin Islands, northeastern Caribbean, from GPS geodesy. Tectonics 6:1021–1037

Jany I, Scanlon KM, Mauffret A (1990) Geological interpretation of combined Seabeam, Gloria and seismic data from Anegada Passage (Virgin Islands, north Caribbean). Mar Geophys Res 12:173–196. doi:10.1007/BF02266712

Jibson RW (1986) Evaluation of landslide hazards resulting from the 5–8 October 1985 storm in Puerto Rico. US Geological Survey Open-File Report 86–26

Jibson RW (1989) Debris flows in southern Puerto Rico. Geol Soc Am Spec Pap 236:29–55

Joyce J, McCann WR, Lithgow C (1987) Onland active faulting in the Puerto Rico platelet: Eos (Transactions, American Geophysical Union) 68: 1483

Kedar S, Hajj GA, Wilson BD, Heflin MB (2003) The effect of the second order GPS ionospheric correction on receiver positions. Geophys Res Lett 30(16):1144–1146

Kouba J (2005) A possible detection of the 26 December 2004 great Sumatra–Andaman Islands earthquake with solution products of the int. GNSS service. Stud Geophys Geod 49:463–483

Kouba J, Springer T (2001) New IGS station and satellite clock combination. GPS Solut 4(4):31–36

Lander JF, Whiteside LS, Lockridge PA (2002) A brief history of tsunamis in the Caribbean Sea. Sci Tsunami Hazards 20(2):57–94

Larson KM, Freymueller JT, Philipsen S (1997) Global plate velocities from the Global Positioning System. J Geophys Res 102:9961. doi:10.1029/97JB00514

Lee S, Kouba J, Schutz B, Kim DH, Lee YJ (2013) Monitoring precipitable water vapor in real-time using global navigation satellite systems. J Geod 87:923–934

Lithgow C, McCann WR, Joyce J (1987) Extensional tectonics at the eastern edge of the Puerto Rico platelet. Eos (Washington, DC). 44: 1483

Liu H, Wang G (2015) Relative motion between St. Croix and the Puerto Rico-Northern Virgin Islands (PRNVI) block derived from continuous GPS observations (1995–2014). Int J Geophys. doi:10.1155/2015/915753

Loureiro P (2014) Cenozoic basin evolution of the Virgin Islands basin and Anegada Passage, northeastern Caribbean. MS thesis, Department of Earth and Atmospheric Sciences, University of Houston

Lyard F, Lefevre F, Letellier T, Francis O (2006) Modelling the global ocean tides: modern insights from FES2004. Ocean Dyn 56(5–6):394–415

Mann P, Burke K (1984) Cenozoic rift formation in the northern Caribbean. Geology 12:732–736. doi:10.1130/0091-7613(1984)12

Mann P, Calais E, Ruegg JC, DeMets C, Jansma PE, Mattioli GS (2002) Oblique collision in the northeastern Caribbean from GPS measurements and geological observations. Tectonics. doi:10.1029/2001TC001304

Mann P, Prentice CS, Hippolyte J-C, Grindlay NR, Abrams LJ, Laó-Dávila D (2005) Reconnaissance study of Late Quaternary faulting along Cerro Goden fault zone, western Puerto Rico. Geol Soc Am Spec Pap 385:115–137. doi:10.1130/0-8137-2385-X.115

Masson DG, Scanlon KM (1991) The neotectonic setting of Puerto Rico. Geol Soc Am Bull 103:144–154

Matthews J, Holcombe T (1976) Possible Caribbean underthrusting of the Greater Antilles along the Muertos trough. 7th Carib. Geol Conf Guadeloupe 235–242

Mattioli GS, Braun JJ, Calais E, Dausz K, Feaux K, Friesen BT, Miller MM, Normandeau J, Seider E, Wang G (2012) COCONet (Continuously Operating Caribbean GPS Observation Network): goals, network status, revised scope, and project highlights. Abstracts and Program SIRGAS Annual Mtg Concepcion, Chile

McCann WR (1985) On the earthquake hazards of Puerto Rico and the Virgin Islands. Bull Seism Soc Am 75:251–262

Meltzer A (1997) Fault structure and earthquake potential of the Lajas Valley. USGS Technical Abstract, SW Puerto Rico

Meltzer A, Almy C (2000) Fault structure and earthquake potential, Lajas Valley, SW Puerto Rico: Eos (Transactions, American Geophysical Union) 81:F1181

Morel L, Pottiaux E, Durand F, Fund F, Boniface K, de Oliveira PS, Baelen JV (2015) Validity and behavior of tropospheric gradients estimated by GPS in Corsica. Adv Space Res 55(1):135–149

Murphy AJ, McCann WR (1979) Preliminary results from a new seismic network in the northeastern Caribbean. Bull Seism Soc Am 69:1497–1513

Nemec MC (1980) A two-phase model for the tectonic evolution of the Caribbean. Trans 9th Carib. Geol Conf St. Domingo 23–34
Pearson P, Snay R (2013) Introducing HTDP 3.1 to transform coordinates across time and spatial reference frames. GPS Solut 17(1):1–17
Pearson C, McCaffrey R, Elliot JL, Snay R (2010) HDTP 3.0: software for copying with the coordinate changes associated with crustal motion. J Surv Eng 136(2):80–90
Pielke RP Jr, Rubiera J, Landsea Ch, Fernández ML, Klein R (2003) Hurricane vulnerability in Latin America and the Caribbean: normalized damage and loss potentials. Nat Hazards Rev 4(3):101–114
Prentice CS, Mann P (2005) Paleoseismic study of the South Lajas fault: first documentation of an onshore Holocene fault in Puerto Rico. Geol Soc Am Spec Pap 385:215–222. doi:10.1130/0-8137-2385-X.215
Prentice CS, Mann P, Burr G (2000) Prehistoric earthquakes associated with a Late Quaternary fault in the Lajas Valley, southwestern Puerto Rico. EOS 81:F1182
Raussen S, Lykke-Andersen H, Kuijpers A (2013) Tectonics of the Virgin Islands basin, north eastern Caribbean. Terra 25:252–257. doi:10.1111/ter.12033
Ray J, Dong D, Altamimi Z (2004) IGS reference frames: status and future improvements. GPS Solut 8:251–266
Rebischung P, Griffiths J, Ray J, Schmid R, Collilieux X, Garayt B (2012) IGS08: the IGS realization of ITRF2008. GPS Solut 16(4):483–494
Reid HF, Taber S (1920) The Virgin Islands earthquakes of 1867–1868. Bull Seismol Soc Am 10:9–30
Rizos C, Janssen V, Roberts C, Grinter T (2012) Precise Point Positioning: Is the Era of differential GNSS positioning drawing to an end?, TS09B, FIG Working Week 2012, Knowing to manage the territory, protect the environment, evaluate the culture heritage, Rome, Italy, 6–10 May 2012
Roig-Silva CM, Asencio E, Joyce J (2013) The Northwest Trending North Boquerón Bay-Punta Montalva Fault Zone; A Through Going Active Fault System in Southwestern Puerto Rico. Seism Res Lett 84(3):538–550
Silva-Tulla F (1986) The October 1985 landslide at Barrio Mameyes. Ponce, National Academy, Washington, DC
Snay RA (1999) Using HTDP software to transform spatial coordinates across time and between reference frames. Surv Land Inf Syst 59:15–25
Snay RA, Soler T (2000) Modern terrestrial reference systems. Part 2: the evolution of the NAD83. Prof Surv 20(2):16–18
Soler T, Snay RA (2004) Transforming positions and velocities between the International Terrestrial Reference Frame of 2000 and North American Datum of 1983. J Surv Eng 130:49–55. doi:10.1061/(ASCE)0733-9453(2004)130:2(49)
Speed RC, Larue DK (1991) Extension and transtension in the plate boundary zone of the northeastern Caribbean. Geophys Res Lett 18:573–576. doi:10.1029/91GL00394
ten Brink US (2005) Vertical motions of the Puerto Rico Trench and Puerto Rico and their cause. J Geophys Res 110:B06404. doi:10.1029/2004JB003459
ten Brink US, Lopez-Venegas AM (2012) Plate interaction in the NE Caribbean subduction zone from continuous GPS observations. Geophys Res Lett 39:L10304. doi:10.1029/2012GL051485
ten Brink US, Bakun WH, Flores CH (2011) Historical perspective on seismic hazard to Hispaniola and the northeast Caribbean region. J Geophys Res 116:B12318. doi:10.1029/2011JB008497
UNAVCO (2014) Shore Drilled Braced Monument. http://pboweb.unavco.org/dmsdocs/Root%20Folder/PBO%20Operations/Miscellaneous%20Documents/SDBM%20installation.pdf. Accessed 22 Jan 2016
Wang G (2011) GPS landslide monitoring: single base versus network solutions—a case study based on the Puerto Rico and Virgin Islands permanent GPS network. J Geodetic Sci 1(3):191–203. doi:10.2478/v10156-010-0022-3
Wang G (2012) Kinematics of the Cerca del Cielo, Puerto Rico landslide derived from GPS observations. Landslides 9(1):117–130. doi:10.1007/s10346-011-0277-5
Wang G (2013a) Millimeter-accuracy GPS landslide monitoring using precise point positioning with single receiver phase ambiguity resolution: a case study in Puerto Rico. J Geod Sci 3(1):22–31. doi:10.2478/jogs-2013-0001
Wang G (2013b) Teaching high-precision GPS to undergraduates using online processing services. J Geosci Educ 61(2):202–212. doi:10.5408/12-295.1
Wang G, Soler T (2012) OPUS for horizontal subcentimeter-accuracy landslide monitoring: case study in the Puerto Rico and Virgin Islands region. J Surv Eng 133(3):143–153. doi:10.1061/(ASCE)SU.1943-5428.0000079
Wang G, Soler T (2014) Measuring land subsidence using GPS: ellipsoid height versus orthometric height. J Surv Eng 05014004:1–12. doi:10.1061/(ASCE)SU.1943-5428.0000137

Wang G, Phillips D, Joyce J, Rivera FO (2011) The integration of TLS and continuous GPS to study landslide deformation: a case study in Puerto Rico. J Geodetic Sci 1(1):25–34. doi:10.2478/v10156-010-0004-5

Wang G, Joyce J, Phillips D, Shrestha R, Carter W (2013a) Delineating and defining the boundaries of an active landslide in the rainforest of Puerto Rico using a combination of airborne and terrestrial LIDAR data. Landslides 10(4):503–513. doi:10.1007/s10346-013-0400-x

Wang G, Yu J, Ortega J, Saenz G, Burrough T, Neill R (2013b) A stable reference frame for ground deformation study in the Houston metropolitan area Texas. J Geod Sci 3(3):188–202. doi:10.2478/jogs-2013-0021

Wang G, Kearns TJ, Yu J, Saenz G (2014) A stable reference frame for landslide monitoring using GPS in the Puerto Rico and Virgin Islands region. Landslides 11(1):119–129. doi:10.1007/s10346-013-0428-y

Wang G, Bao Y, Cuddus Y, Jia X, Serna J, Jing Q (2015) A methodology to derive precise landslide displacement time series from continuous GPS observations in tectonically active and cold regions: a case study in Alaska. Nat Hazards 77(3):1939–1961. doi:10.1007/s11069-015-1684-z

Yang L, Wang G, Bao Y, Kearns TJ, Yu J (2015) Comparisons of ground-based and building-based CORS: a case study in the Puerto Rico and the Virgin Islands. J Surv Eng. doi:10.1061/(ASCE)SU.1943-5428.0000155

Zumberge JF, Heflin MB, Jefferson DC, Watkins MM, Webb FH (1997) Precise point positioning for the efficient and robust analysis of GPS data from large networks. J Geophys Res 102(B3):5005